

This work has been submitted to the IEEE for possible publication. Copyright may be transferred without notice, after which this version may no longer be accessible.

arXiv:1901.05494v2 [eess.SP] 10 Jan 2020

# Optimizing IoT Energy Efficiency on Edge (EEE): a Cross-layer Design in a Cognitive Mesh Network

Jianqing Liu, Yawei Pang, Haichuan Ding, Ying Cai, Haixia Zhang, Yuguang Fang

**Abstract**—Battery-powered wireless IoT devices are now widely seen in many critical applications. Given the limited battery capacity and inaccessibility to external power recharge, optimizing energy efficiency (EE) plays a vital role in prolonging the lifetime of these IoT devices. However, a sheer amount of existing works only focus on the EE design at the infrastructure level such as base stations (BSs) but with little attention to the EE design at the device level. In this paper, we propose a novel idea that aims to shift energy consumption to a grid-powered cognitive radio mesh network thus preserving energy of battery-powered devices. Under this line of thinking, we cast the design into a cross-layer optimization problem with an objective to maximize devices' energy efficiency. To solve this problem, we propose a parametric transformation technique to convert the original problem into a more tractable one. A baseline scheme is used to demonstrate the advantage of our design. We also carry out extensive simulations to exhibit the optimality of our proposed algorithms and the network performance under various settings.

**Index Terms**—Energy efficiency, Cognitive radio network, OFDM, Cross-layer optimization, Fractional programming.

## I. INTRODUCTION

Over the last few years, the explosive growth of smart devices is accelerating the advent of Internet-of-Things (IoT). Among these IoT devices, a significant number of them run on wireless radio and are powered by battery [1], [2]. It is simply because they are deployed in hard-to-access locations, infeasible to be hard wired, or just designed to be user friendly. Such use cases sometimes require battery-powered IoT devices to operate for a significant amount of time without battery replacement, 10 years for instance [3]. To achieve this goal, a few low-power wireless technologies such as Bluetooth Low Energy (BLE) [4], ZigBee (IEEE 802.15.4e) [5], WiFi (IEEE 802.11ah) [6], low-power long-range (LoRa) [7] are developed with the objective of optimizing a device's radio interface for higher energy efficiency (e.g., via better power control and transmission scheduling). However, such optimization with

energy efficiency as the objective usually comes with the sacrifice to other metrics. For instance, long duty-cycle incurs high latency [8]; low transmit power reduces data rate [9] and simplified radio even hampers security [10]. In light of this, alternative solutions to increasing IoT devices' energy efficiency are worthwhile to investigate.

It has been well recognized that the attempt in increasing energy efficiency is constrained by the spectrum efficiency [11]. The reason lies in the Shannon's capacity theorem, which reveals that link capacity increases only logarithmically with power but linearly with bandwidth, indicating that bandwidth could more effectively bring down the power consumption. With the observation that a large portion of licensed spectrum is not well utilized in certain areas [12], one can harvest and opportunistically access under-utilized spectrum. As an enabling technology, cognitive radio (CR) [13] promises to realize dynamic spectrum access and thus increase spectrum efficiency.

In this paper, we propose a novel idea - by allowing battery-powered IoT devices to shift their energy consumption to grid-powered CR-capable devices, IoT devices' energy efficiency can be increased. This energy-efficiency-on-edge (EEE) idea is motivated by the observation that IoT devices are more sensitive to energy consumption than grid-powered devices are. In other words, it is worthwhile to spend a bit more grid energy on grid-powered devices so as to somewhat, if not significantly, improve the energy efficiency of battery-powered devices. To enable such "energy shift", we leverage a cognitive capacity harvesting network (CCHN) which was firstly proposed in our previous works [14] as shown in Fig.1. The essence of this architecture is that the routers, also called CR routers, have CR capabilities and they can form a multi-hop mesh network to get closer to and help the end devices with no CR capabilities for data exchange, potentially saving energy and increasing spectrum efficiency. Under this structure, we intend to augment it with a centralized IoT system<sup>1</sup> (e.g., LoRAWAN, LTE) and let the CCHN help battery-powered IoT devices to relay data, thus increasing their energy efficiency.

Specifically, we consider the uplink transmission where IoT devices can send data either directly to the BS/gateway or to CR routers. For the former case, it is a one-hop transmission while in the latter one, an IoT device is firstly connected to a CR router using its existing radio interface (e.g., LoRa, WiFi) and its traffic are then delivered to the BS via multi-hop

J. Liu is with the Department of Electrical and Computer Engineering, University of Alabama in Huntsville, Huntsville, AL 35899 USA e-mail: jianqing.liu@uah.edu

Y. Pang is with the Department of IoT, School of Computer and Software, Nanjing University of Information Science and Technology, Nanjing 210044, China e-mail: yaweipang@gmail.com

H. Ding is with the Department of Electrical Engineering and Computer Science, University of Michigan, Ann Arbor, MI 48109 USA e-mail: dhcbit@gmail.com

Y. Cai is with the Computer School, Beijing Information Science & Technology University, Beijing 100101, China e-mail: ycai@bistu.edu.cn

H. Zhang is with the School of Control Science and Engineering, Shandong University, Jinan 250100, China e-mail: haixia.zhang@sdu.edu.cn

Y. Fang is with the Department of Electrical and Computer Engineering, University of Florida, Gainesville, FL 32611 USA e-mail: fang@ece.ufl.edu.

<sup>1</sup>In this work, a hypothetical model instead of a realistic system is used to convey the idea.

transmissions using harvested bands. The rationale of studying this problem is that IoT devices could use lower transmission power to associate with closer CR routers but may not be able to always receive satisfactory service through the CCHN due to the uncertainty of the harvested bands; while they could obtain reliable throughput via direct connection to the BS but may need to apply higher transmission power. Obviously, there is a tradeoff between service quality (i.e., reliability and throughput) and power consumption. Therefore, we will investigate the energy efficient design in this respect, with the design dimension to be device association, uplink power control and channel allocation, and multi-hop scheduling and routing in the CCHN.

Towards this design objective, there are several technical challenges to be addressed. First, the weighted sum-of-ratios form of the objective function is non-convex, which makes the optimization problem difficult to tackle. Second, the availability of harvested spectrum is highly unpredictable and the usable bandwidth in this regard should be naturally modeled as a random variable, which results in a stochastic constraint and makes the problem intractable. Third, the association variable is in integer form and tightly coupled with other decision variables so solving the problem via conventional approaches is highly prohibitive especially when the network size is large. In light of these aforementioned challenges, we propose corresponding solution to each of them, which in turn demonstrates our technical contributions as follows:

- We introduce auxiliary variables and transform the original objective function into a parametric subtractive form which bears the desired convexity property. Their equivalence in terms of finding the same solution is further proved.
- We reformulate the stochastic constraint of the availability of harvested spectrum as a chance constraint of  $\Delta$ -confidence level. Then, the feasible region of original optimization problem becomes a convex set.
- We address the integer programming part through a two-step procedure: relaxing and then rounding. To decouple the decision variables, we further apply the dual-based approach to make the original problem more tractable.

The rest of the paper is organized as follows. Section II introduces the most recent literature of this topic. Section III describes the system model. The problem formulation is outlined in Section IV. We propose solution algorithms in Section V and present the performance evaluation in Section VI. Finally, Section VII concludes the paper.

## II. RELATED WORKS

IoT wireless access technology can be broadly classified into random access (or contention-based) and deterministic access (or connection-based) categories [15]. Exemplary standard of the former is LTE-RACH [16] while the latter could be TDMA-based (e.g., BLE) and OFDM-based (e.g., 802.11ah). There has been a flux of works on optimizing these standards to make them energy-efficient, but the drawbacks are also evident in the sense that other performance metrics such as latency, throughput and security could be hampered [8],

[9], [10]. Since our work is not constrained to any existing standard, we will survey generic EE design in hypothetical wireless networks. Nevertheless, the number of related works is still significant so we limit the scope to the OFDM-based access systems and future networks like cognitive radio networks (CRNs) and the CRN-enabled networks.

The well-recognized EE design model is to maximize energy efficiency (defined as the ratio of rate to power consumption) under wireless resource constraints [17]. For instance, in an OFDM-based radio access network, there are many related works to optimize EE by jointly considering power control and subcarrier allocation [18], [19], [20], [21]. Cheung *et al.* [18] focused on a multi-relay assisted OFDM cellular network and studied the EE maximization problem by formulating EE as the ratio of total network throughput to total power consumption at a BS. Xiong *et al.* also targeted at the same wireless setting but investigated the EE maximization constrained on users' proportional rate fairness [19]. However, these papers and their related ones bear two major shortcomings: (i) they modeled the network EE in a "sum-to-sum" form (instead of the "sum-of-ratios" form) which fails to capture each device's EE; (ii) they used the infrastructure's power consumption in calculating EE, which lacks emphasis on the battery-powered end devices. Unfortunately, there is a lack of study when it comes to addressing these two issues. Recent works [20], [21] nonetheless have some merits along this line. Zarakovitis *et al.* [21] studied the EE design in a downlink OFDM cellular system by characterizing EE in weighted sum-of-ratios. They applied the Maclaurin series expansion to transform the objective into a tractable form and then solved it in polynomial time. He *et al.* [20] focused on a multi-cell downlink OFDM cellular system with coordinated beamforming. They introduced auxiliary variables to transform the weighted sum-of-ratios objective into a parametric subtractive form, which afterwards became easier to address. These works adopted the "sum-of-ratios" to define the EE objective but still employed the infrastructure's rather than the device's power consumption.

The EE design in CRNs and CRN-enabled networks is still in its infancy. Amongst the limited works, Wang *et al.* in [22] considered an OFDM-based CRNs and investigated the EE design by taking channel uncertainty into consideration. Xie *et al.* [23] proposed a new cognitive cellular network architecture consisting of macrocells and femtocells. They utilized game theoretic approaches to investigate the energy efficient resource allocation. There are other similar works in this context [24], [25], but they all bear two critical limitations: (i) end devices are assumed to have CR capabilities which in nature is not energy efficient due to the tedious spectrum sensing; (ii) the EE measurement is the ratio of overall rate to overall power consumption, which is in the "sum-to-sum" form. To cope with the first challenge, a cognitive capacity harvesting network (CCHN) was proposed in [14] and its basics are discussed in Section II. Under this architecture, Ding *et al.* [26], [27] and Liu *et al.* [28], [29] developed protocols to achieve higher throughput and energy efficiency for lightweight end devices.

In this work, we exploit the CCHN-enabled OFDM access

system to maximize energy efficiency of battery-powered IoT devices. We characterize the network EE using the summation of end devices' EE, and model the problem under a novel idea - "energy shift" from battery-powered devices to grid-powered ones.

### III. SYSTEM MODEL

#### A. Network Description

In this paper, we consider a CCHN-augmented network which consists of a secondary service provider (SSP), a BS, multiple CR routers and end users<sup>2</sup>, as shown in Fig.1. Specifically, SSP is a wireless service provider which has its own licensed bands, typically called the "basic bands", for reliable control signalling, handling handovers and so on. SSP could also harvest spectrum bands from other operators via paradigms such as spectrum sensing or spectrum auction. As the centralized coordinator, SSP observes and collects network information (e.g., users' traffic demands, channel state information) in its coverage area and then performs network optimization (e.g., power control, channel allocation, link scheduling and routing) to determine the optimal approaches for service provisioning. CR routers are grid-powered devices with CR capabilities, and they form a mesh network that is capable of using the harvested bands to transmit data. BS has multiple radio interfaces and serves as the gateway to the Internet for CR routers. In this architecture, end users do not have to possess CR capabilities. CR routers could tune their radio interfaces to what end users use to make connections. Due to the close proximity between CR routers and end users, the frequency reuse ratio and devices' energy efficiency are greatly enhanced. For more details of this architecture, interested readers are referred to [14].

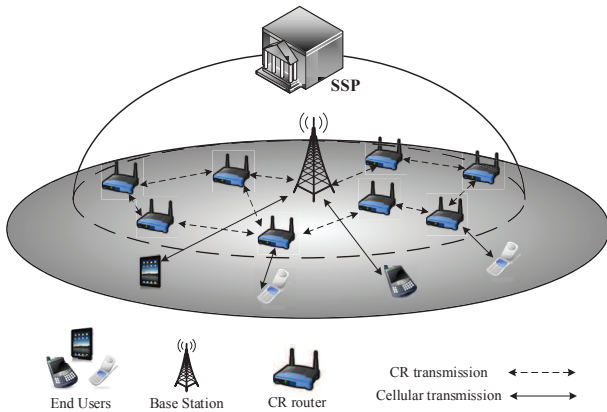


Figure 1: The CCHN-augmented IoT Network.

#### B. Network model

In this paper, we focus on uplink data transmission from IoT devices to a BS. As shown in Fig.1, suppose a set of battery-powered devices/users, say,  $\mathcal{U} = \{1, \dots, u, \dots, U\}$ ,

<sup>2</sup>We use "end users" and "IoT devices" interchangeably in the following article to represent the same meaning.

each of which initializes a session whose destination is the BS denoted by  $b$ . We index the set of sessions as  $\mathcal{L} = \{l_1, \dots, l_u, \dots, l_U\}$  and let  $s(l_u)$  and  $d(l_u)$  denote the source (i.e.,  $s(l_u) = u$ ) and destination (i.e.,  $d(l_u) = b$ ) of session  $l_u \in \mathcal{L}$ , respectively. Also consider the network consisting of  $K$  CR routers  $\mathcal{K} = \{1, \dots, k, \dots, K\}$  and together with the BS  $b$ , we denote  $\overline{\mathcal{K}} = \mathcal{K} \cup \{b\}$  as the set of grid-powered wireless infrastructures. Suppose the network applies single carrier-frequency division multiplexing access (SC-FDMA) for end users' uplink transmissions, where the network's basic band is divided into  $N_{tot}$  number of orthogonal sub-channels which are shared among end users. Denote the harvested band as  $m$  and it is allocated to the mesh network to form multi-hop transmissions.

Our model is applicable to a low mobility scenario. In such an environment, resource allocation can be conducted during the channel coherence time when channel is regarded as static. In light of this, we can just apply the line-of-sight (LOS) channel model instead of fast fading ones. Moreover, although signaling and computation overhead is incurred when solving the cross-layer optimization problem, the solution is applicable over a relatively long time scale due to users' low mobility and small variation of network parameters, which makes such overhead tolerable in the long run.

### IV. PROBLEM FORMULATION

Given the system model described before, we target at the problem of uplink end-to-end data delivery from end users to the BS, where the user association, uplink power control, channel allocation, routing and link scheduling are jointly considered so as to maximize the network wide end users' energy efficiency.

#### A. Uplink SC-FDMA

In practical systems, similar to specifications in the 3GPP LTE standard, the uplink SC-FDMA in our design also implies restrictions on power and channel allocation [30]. First, any sub-channel can only be assigned to one user, called *exclusiveness*. Second, every user's allocated sub-channels must be continuous, called *adjacency*. Third, user's transmit power should be identical on any allocated sub-channel in order to retain a low peak-to-average power ratio (PAPR).

Denote the indicator  $x_{u,k}$  as the association variable, where  $x_{u,k} = 1$  implies that user  $u$  is associated with infrastructural node  $k$ , and  $x_{u,k} = 0$  otherwise. Normally, the association is assumed to be performed in a large scale compared to the variation of channel so the fast fading is averaged out over the association time [31]. We also consider a relatively low mobility environment, where the resource allocation is carried out during the channel coherence time so the channel can be regarded as static. Furthermore, in our network, to simplify the problem, we assume the  $N_{tot}$  sub-channels are not reused so as to avoid strong interference.

1) *User Association*: Any end user can only be associated with the BS or a CR router, but not both. This physical constraint can be expressed as follows

$$\sum_{k \in \mathcal{K}} x_{u,k} = 1, \quad \forall u \in \mathcal{U}, \quad (1)$$

$$x_{u,k} \in \{0, 1\}, \quad \forall u \in \mathcal{U}, \forall k \in \mathcal{K}. \quad (2)$$

2) *Sub-channel Allocation*: Suppose the end user  $u$  is allocated with  $N_u$  number of sub-channels which are contiguous in nature<sup>3</sup>. Due to the property of *exclusiveness*, the total allocated sub-channels cannot exceed  $N_{tot}$ , which is stated in below

$$\sum_{u \in \mathcal{U}} N_u \leq N_{tot}, N_u \in \mathbb{Z}^+ \quad (3)$$

where  $\mathbb{Z}^+$  denotes the set of nonnegative integers.

3) *Link Capacity*: Given the sub-channel allocation, according to Shannon-Hartley theorem, the capacity of the link between an end user  $u$  and the infrastructural node  $j$  can be calculated as follows

$$c_{u,j} = N_u W \cdot \log_2 \left( 1 + \frac{p_u |h_{u,j}|^2}{N_u W \cdot N_0} \right), \forall u \in \mathcal{U}, \forall j \in \mathcal{K}, \quad (4)$$

where  $W$  is the bandwidth of each sub-channel,  $N_0$  is the power spectrum density (of unit  $W/Hz$ ) of the Additive White Gaussian Noise (AWGN), and  $h_{u,k}$  is the channel fading coefficient. Here,  $p_u$  is denoted as the transmit power of the end user  $u$  and as we know,  $p_u$  must be evenly distributed across the allocated sub-channels to retain a low PAPR, which is given by  $\frac{p_u}{N_u}$ . Therefore, the link capacity is calculated as the sum of all allocated sub-channels' capacities, as shown in (4).

4) *Power Control*: Due to the hardware constraint, the transmit power of an end user cannot exceed its maximum allowable power level  $P_{u,max}$ . Since end users have different power capabilities,  $P_{u,max}$  is a user-dependent variable. Moreover, we do not consider the power control of CR routers so their transmit powers are assumed to be fixed.

## B. The Cognitive Mesh Network

When an end user is associated with a CR router, its traffic is delivered to the BS via multi-hop transmissions in the cognitive mesh network. In other words, the SSP allocates the harvested band  $m$  to the mesh network and performs link scheduling and routing optimization to determine how to assist the end user  $u$  to complete its session  $l_u$  whose destination is the BS  $b$ . In what follows, we investigate the link scheduling and routing problem in the cognitive mesh network.

1) *Transmission Range and Interference Range*: Following the widely used model [26], we define the power propagation gain from the CR router  $i$  ( $\forall i \in \underline{\mathcal{K}}$ ) to another infrastructural node (either a CR router or the BS)  $j$  ( $\forall j \in \mathcal{K} \setminus i$ ) as  $g_{i,j} = \zeta \cdot d_{i,j}^{-\gamma}$ , where  $\zeta$  is the antenna gain,  $d_{i,j}$  refers to the Euclidean distance between  $i$  and  $j$ , and  $\gamma$  is the path loss exponent.

<sup>3</sup>Note that our work can be naturally extended to incorporate the case of finding the optimal sub-channel allocation pattern (i.e., a specific chunk of  $N_u$  sub-channel collections) [32], [33], and we will leave it for the future work.

Let assume that CR routers apply the same constant transmit power  $P_t$  and define that the transmission is successful only when the received signal power exceeds a threshold  $P_r^{th}$ , i.e.,  $P_t \cdot g_{i,j} \geq P_r^{th}$ . Then, we can obtain the transmission range of CR router  $i$  as  $R_i^t = (P_t \cdot \zeta / P_r^{th})^{1/\gamma}$ . Accordingly, we define the set of infrastructural nodes being in the transmission range of the CR router  $i$  ( $\forall i \in \underline{\mathcal{K}}$ ) as

$$\mathcal{T}_i = \{j \in \mathcal{K} | d_{i,j} \leq R_i^t, j \neq i\}. \quad (5)$$

On the other hand, to efficiently use harvested bands, the SSP should ensure the transmissions over different links do not conflict with each other. In light of this, we define the interference range in a similar way as before. Suppose the received interference can be ignored only when the received power is less than a threshold  $P_I^{th}$ , i.e.,  $P_t \cdot g_{i,j} < P_I^{th}$ . Therefore, the interference range of the CR router  $i$  ( $\forall i \in \underline{\mathcal{K}}$ ) can be obtained as  $R_i^I = (P_t \cdot \zeta / P_I^{th})^{1/\gamma}$ . Accordingly, the set of infrastructural nodes being in the interference range of the CR router  $i$  ( $\forall i \in \underline{\mathcal{K}}$ ) is defined as

$$\mathcal{I}_i = \{j \in \mathcal{K} | d_{i,j} \leq R_i^I, j \neq i\}. \quad (6)$$

2) *Conflict Graph and Independent Sets* [26]: Given the prior definition of the interference range, we can claim that two communication links conflict if the receiver of one link is within the interference range of the transmitter of the other link. A conflict graph  $G = (V, E)$  is used to characterize the interfering relationship among different infrastructural links. Specifically, each vertex  $v$  indicates a transmission link  $(i, j)$  ( $\forall i \in \underline{\mathcal{K}}, \forall j \in \mathcal{K} \setminus i$ ) and two links are said to be conflicted if there is an edge  $e$  connecting the two corresponding vertices.

With this conflict graph being created, we can define an independent set (IS), which consists of a set of vertices  $I \subseteq V$  and any two of them do not share an edge. In this case, all the transmission links in an IS do not interfere with each other and thus can be carried out successfully at the same time. If adding one more vertex into the IS  $I$  results in a non-independent one, the set  $I$  is called the maximal independent set (MIS). We can collect all the MISs of the conflict graph in a set  $\mathcal{Q} = \{I_1, \dots, I_q, \dots, I_Q\}$ , where  $Q$  represents the total number of MISs, i.e.,  $Q = |\mathcal{Q}|$ .

3) *Link Scheduling*: In this paper, we consider different MISs are scheduled with certain time shares (out of unit time) so that the links within each MIS can carry out the transmissions simultaneously. From our previous discussion, we know only one of the MISs can be active at one time instance and we denote the time share allocated to the MIS  $I_q$  as  $\lambda_q$ . Therefore, we have to satisfy the following constraint

$$\sum_{q=1}^Q \lambda_q \leq 1, \quad (7)$$

$$0 \leq \lambda_q \leq 1, \forall q \in \{1, \dots, Q\}. \quad (8)$$

On the other hand, the link capacity of the link  $(i, j)$  can be obtained based on Shannon-Hartley theorem, which is

$$c_{i,j} = W_m \cdot \log_2 \left( 1 + \frac{P_t \cdot g_{i,j}}{W_m \cdot N_0} \right), \forall i \in \underline{\mathcal{K}}, \forall j \in \mathcal{K} \setminus i, \quad (9)$$

where  $W_m$  is the bandwidth of the harvested band. According

to the link scheduling, the actual data rate over the link  $(i, j)$  could be 0 if  $(i, j)$  is not scheduled at a time instance. In other words, we use  $r_{i,j}(I_q)$  to represent the achieved data rate over the link  $(i, j)$  when  $I_q$  is scheduled, where  $r_{i,j}(I_q) = c_{i,j}$  if  $(i, j) \in I_q$  and 0 otherwise. Considering the link  $(i, j)$  could exist in all the MISs, the total achieved data rate over the link  $(i, j)$  can be expressed as

$$R_{i,j} = \sum_{q=1}^Q \lambda_q r_{i,j}(I_q). \quad (10)$$

4) *Flow Routing*: In this paper, we consider the network level end-to-end (from users to the BS) service provisioning. Suppose the end user  $u$  initiates a session  $l_u$ , the SSP should determine whether to support it by associating  $u$  directly to the BS through one-hop transmission or connecting  $u$  to the cognitive mesh network and then arriving at the BS via multi-hop transmissions. Here denote  $f_{i,j}(l_u)$  as the supported flow rate for the session  $l_u$  over the link  $(i, j)$  at the network level. If node  $i$  is the source of session  $l_u$ , which is the end user  $u$  (i.e.,  $s(l_u) = u$ ), we have the following constraints

$$\sum_{j \in \{j|u \in \mathcal{T}_j\}} f_{j,u}(l_u) = 0, \quad (11)$$

$$f_{u,j}(l_u) \cdot x_{u,j} = r(l_u). \quad (12)$$

The constraint (11) means that the incoming flow rate of any session at the source node is zero since the end user is the initiator of the session. The constraint (12) reflects the first hop from the end user  $u$  to an infrastructural node  $j \in \mathcal{K}$ , where  $r(l_u)$  signifies the achievable data rate of user  $u$ . Clearly, the association variable is coupled with flow rate in (12), implying that there only exists one wireless link from the end user  $u$  to one of the infrastructural nodes to support  $u$ 's data rate. Besides, the flow rate on a link should be constrained by the link capacity according to (4), which is expressed as

$$0 \leq f_{u,j}(l_u) \leq c_{u,j}. \quad (13)$$

For any infrastructural node  $i \in \mathcal{K}$ , which is the CR router, the flow conservation law (FCL) implies that for any session  $l_u$ , the total flow into  $i$  must be equal to the total flow out of  $i$ . This can be expressed as

$$\sum_{j \in \{j|i \in \mathcal{T}_j\}} f_{j,i}(l_u) + f_{u,i}(l_u) \cdot x_{u,i} = \sum_{k \in \mathcal{T}_i} f_{i,k}(l_u). \quad (14)$$

Clearly, if the CR router  $i$  is directly associated with end user  $u$ , constraint (14) could be rewritten as  $r(l_u) = \sum_{k \in \mathcal{T}_i} f_{i,k}(l_u)$  according to (12); whereas if the CR router  $i$  is the intermediate infrastructural node to support  $l_u$ , constraint (14) would be equivalent to  $\sum_{j \in \{j|i \in \mathcal{T}_j\}} f_{j,i}(l_u) = \sum_{k \in \mathcal{T}_i} f_{i,k}(l_u)$ .

Moreover, all the flows in the cognitive mesh network are completed at the BS, which means that the BS is the common destination, i.e.,  $d(l_u) = b, \forall l_u \in \mathcal{L}$ . Thus, we have another constraints for the destination node  $b$  described as follows:

$$\sum_{j \in \mathcal{T}_b} f_{b,j}(l_u) = 0, \quad (15)$$

$$f_{u,b}(l_u) \cdot x_{u,b} + \sum_{j \in \{j|b \in \mathcal{T}_j\}} f_{j,b}(l_u) = r(l_u). \quad (16)$$

Note that if the end user  $u$  is directly connected to the BS (i.e.,  $x_{u,b} = 1$ ), (16) becomes  $\sum_{j \in \{j|b \in \mathcal{T}_j\}} f_{j,b}(l_u) = 0$ , indicating that session  $l_u$  is not supported through the CR routers. Instead, if  $x_{u,b} = 0$ , meaning user  $u$  is associated with the cognitive mesh network, (16) could be rewritten as  $\sum_{j \in \{j|b \in \mathcal{T}_j\}} f_{j,b}(l_u) = r(l_u)$ .

Besides, for the link from one CR router  $i \in \mathcal{K}$  to another infrastructural node  $j \in \mathcal{T}_i$ , the total flow rate on that link (by aggregating all the rates of supported sessions) should not exceed the link capacity. From our previous discussion, we know that the link capacity is dependent on the scheduled time share on that link, which is described as (10). Thus, we have the following constraint

$$0 \leq \sum_{l_u \in \mathcal{L}} f_{i,j}(l_u) \leq R_{i,j}. \quad (17)$$

### C. User-centric Network-wide Energy Efficiency Optimization

Our work aims to maximize the user-centric network-wide (i.e., the weighted sum of end users') energy efficiency by considering user diversity in power capability (e.g., residual energy, maximal allowable power). In light of it, we apply the ratio-based EE model, where the EE is measured in bit/s/Joule and defined as the ratio of data rate to power consumption which in this work are both with respect to the end users. Thus, we coin it as the user-centric EE metric, in contrast to the previous works that applied BS's power consumption in the EE definition [20], [21]. Furthermore, contrary to the conventional EE definition as the ratio of the system sum rate to the sum power consumption [18], [34], our user-centric network-wide EE measures the weighted sum of end users' EE, such that the heterogeneous EE requirements from different users of various power capabilities can be investigated.

Before presenting the optimization problem, we first define the power consumption model of end user  $u$  as  $\eta p_u + P_c$ , where  $\eta$  is the efficiency of the transmit power amplifier when it operates in the linear region, whereas  $P_c$  is the circuitry power dissipated in all other circuit blocks (e.g., mixer, oscillator, DAC and etc.) which is independent of the transmit power  $p_u$  and normally a constant value. Then, the EE for the end user  $u$  can be obtained as  $\frac{r(l_u)}{\eta p_u + P_c}$ , where  $r(l_u)$  denotes its achieved data rate according to (12). Finally, we introduce a weighting factor  $\omega_u$  associated with user  $u$ 's EE, which provides a means for service differentiation as well as fairness. Particularly, the weights could be determined inversely proportional to users' residual energy so that less power capable users are allocated with higher EE priorities.

By considering the user association, power control, channel allocation, routing and link scheduling constraints introduced previously, we can thus formulate the following optimization problem to achieve the maximal User-centric Network-wide

## EE (UNEE-Max)

$$\begin{aligned}
& \text{Max} \quad \sum_{u \in \mathcal{U}} \omega_u \frac{r(l_u)}{\eta p_u + P_c} \\
& \text{s.t.} \quad (1) \sim (3), (7) \sim (8), (11) \sim (17); \\
& \quad 0 \leq f_{i,j}(l_u), \forall l_u \in \mathcal{L}, \forall i \in \mathcal{K}, \forall j \in \mathcal{K} \setminus i; \\
& \quad 0 \leq p_u \leq P_{u,\max}, \forall u \in \mathcal{U}
\end{aligned} \tag{18}$$

where  $x_{u,k}$ ,  $N_u$ ,  $p_u$ ,  $f_{u,j}(l_u)$ ,  $f_{i,j}(l_u)$  and  $\lambda_q$  are optimization decision variables. Clearly, UNEE-Max is a cross-layer optimization problem involving coupled variables from the physical layer to the network layer. In the next section, we elaborate several difficulties in addressing UNEE-Max problem and introduce techniques to solve it accordingly.

## V. OVERVIEW OF THE UNEE-MAX PROBLEM

### A. Complexity of The UNEE-Max

We first highlight several key difficulties in solving the UNEE-Max problem.

1) *NP-completeness for searching all MISs*: Under constraint (7), we need to search all the MISs for link scheduling. However, finding all the MISs in a conflict graph  $G = (V, E)$  is NP-complete, which is the common obstacle encountered in multi-hop wireless networks [35]. Although we can apply brute-force search when the size of  $G = (V, E)$  is small, it is highly prohibitive when  $G$  becomes large. Therefore, it requires a cost-effective approach to find MISs so as to make the problem tractable.

2) *Uncertainty of the harvested band*: In CRNs, SUs are allowed to access PUs' spectrum bands only when these bands are not occupied by PUs. SUs must immediately evacuate when PUs reclaim the spectrum. In practice, the availability of these harvested bands is highly unpredictable due to the uncertainty of PUs' activity and SSP's statistical inference model (i.e., false alarm / miss detection probabilities) [36]. Therefore, the bandwidth  $W_m$  of the harvested band (defined in (9)) is a random variable, whose probability distribution could be derived from statistical characteristics of these PUs' bands from some observations and experiments [37]. However, the randomness of  $W_m$  makes (17) a stochastic constraint, which causes the feasible region of UNEE-Max to be both random and nonconvex.

3) *Combinatorial nature of user association*: The indicator variable  $x_{u,k}$  in constraints (1) and (2) enforces unique association, which makes the problem combinatorial. Although the classical branch-and-bound approach can be applied to solve general integer programming problems, due to the tight coupling between the association and the resource allocation (i.e., power control, link scheduling and routing) in UNEE-Max, it is difficult to solve using traditional approaches.

4) *Nonconcavity of objective function*: The objective function in the UNEE-Max problem is in the form of weighted sum of linear fractional functions (WSolFF), which is generally nonconcave [38]. An immediate consequence is that the powerful tools from the convex optimization theory do not apply to the UNEE-Max, and the KKT conditions are only necessary conditions for optimality [39]. Therefore, we need

to transform the UNEE-Max to a certain form from which approximate solution to the UNEE-Max can be found.

### B. The UNEE-Max Relaxation Algorithm

After outlining the difficulties in solving UNEE-Max problem, we introduce the relaxation or transformation techniques to make the UNEE-Max tractable.

1) *Critical MIS set*: Although there exists exponentially many MISs in a conflict graph, Li *et. al.* [35] proved that only a small portion of MISs, termed as *critical MIS set*, can be scheduled in the optimal resource allocation. Instead of searching all MISs, we thus apply the SIO-based approach proposed in [35], [40] to return the critical MIS set  $\mathcal{Q}' = \{I_1, \dots, I_q, \dots, I_{Q'}\}$  in polynomial time, where  $\mathcal{Q}' \subseteq \mathcal{Q}$ . Therefore, we can replace  $\mathcal{Q}$  with  $\mathcal{Q}'$  in constraint (1), and (17) to make the UNEE-Max problem more tractable. Note that SIO-based approach may only give a fraction of  $\mathcal{Q}'$  in a limited searching time leading to a loss in solution optimality. In light of this, we could deliberately allow a longer searching time as the SIO-based approach can be run offline.

2)  *$\Delta$ -confidence level*: To address the stochastic constraint (17), inspired by the concept of value at risk (VaR) in [41], we reformulate it as a chance constraint of  $\Delta$ -confidence level represented as follows

$$\Pr \left[ 0 \leq \sum_{l_u \in \mathcal{L}} f_{i,j}(l_u) \leq \sum_{q=1}^{\mathcal{Q}} \lambda_q W_m \log_2 \left( 1 + \frac{P_t \cdot g_{i,j}}{W_m N_0} \right) \right] \geq \Delta,$$

where  $\Delta \in [0, 1]$  indicates the confidence level for stochastic constraint (17) to be satisfied and  $(i, j) \in I_q$ . Suppose  $F_{W_m}(\cdot)$  represent the cumulative distribution function (CDF) of random variable (r.v.)  $W_m$ . We could then obtain the  $F_{c_{i,j}}(\cdot)$  as the CDF for the r.v.  $c_{i,j} = W_m \log_2 \left( 1 + \frac{P_t \cdot g_{i,j}}{W_m N_0} \right)$ , which is the link capacity of  $(i, j)$ . Thus, by integrating the critical MISs, the above inequality could be reformulated as

$$0 \leq \sum_{l_u \in \mathcal{L}} f_{i,j}(l_u) \leq \sum_{q=1}^{\mathcal{Q}'} \lambda_q F_{c_{i,j}}^{-1}(1 - \Delta). \tag{19}$$

By replacing (17) with (19), the original stochastic constraint is converted to a linear inequality constraint in  $f_{i,j}(l_u)$  and  $\lambda_q$ .

3) *Integer relaxation and rounding*: In the first phase, we assume that end users can be associated with the BS and CR routers at the same time. In other words, we relax the integer association variable  $x_{u,k}$  to the continuous domain of  $[0, 1]$ . Under this assumption, we also introduce the sub-channel auxiliary variable  $N_{u,k} = N_u \cdot x_{u,k}$ , where  $N_{u,k} \in \mathbb{R}^+$  and  $\mathbb{R}^+$  represents set of all nonnegative numbers, the power auxiliary variable  $p_{u,k} = p_u \cdot x_{u,k}$  and the flow auxiliary variable  $\tilde{f}_{u,k}(l_u) = f_{u,k}(l_u) \cdot x_{u,j}$ , so that  $\sum_{k \in \mathcal{K}} N_{u,k} = N_u$ ,  $\sum_{k \in \mathcal{K}} p_{u,k} = p_u$ ,  $\sum_{k \in \mathcal{K}} \tilde{f}_{u,j}(l_u) = r(l_u)$ . Therefore, we can eliminate association constraint (1) and (2) and rewrite the UNEE-Max problem as

a Relaxed-UNEE-Max problem which is described as follows

$$\begin{aligned}
\text{Max} \quad & \sum_{u \in \mathcal{U}} \omega_u \frac{\sum_{k \in \mathcal{K}} \tilde{f}_{u,k}(l_u)}{\eta \sum_{k \in \mathcal{K}} p_{u,k} + P_c} \\
\text{s.t.} \quad & 0 \leq \sum_{u \in \mathcal{U}} \sum_{k \in \mathcal{K}} N_{u,k} \leq N_{\text{tot}}, N_{u,k} \in \mathbb{R}^+; \\
& 0 \leq \sum_{k \in \mathcal{K}} p_{u,k} \leq P_{u,\text{max}}, \forall u; p_{u,k} \in \mathbb{R}^+; \\
& 0 \leq \tilde{f}_{u,k}(l_u) \leq N_{u,k} W \log_2 \left( 1 + \frac{p_{u,k} |h_{u,k}|^2}{N_{u,k} W N_0} \right), \forall u, \forall k; \\
& \sum_{j \in \{j | i \in \mathcal{T}_j\}} f_{j,i}(l_u) + \tilde{f}_{u,i}(l_u) = \sum_{k \in \mathcal{T}_i} f_{i,k}(l_u), \forall u; \\
& \sum_{j \in \{j | b \in \mathcal{T}_j\}} f_{j,b}(l_u) = \sum_{k \in \mathcal{K}} \tilde{f}_{u,k}(l_u), \forall u; \\
& (7) \sim (8), (11), (15), (19); \\
& 0 \leq f_{i,j}(l_u), \forall l_u \in \mathcal{L}, \forall i \in \mathcal{K}, \forall j \in \mathcal{K} \setminus i.
\end{aligned} \tag{20}$$

In the second phase, we develop a rounding scheme, as what will be discussed in Section VII, to convert the output of the Relaxed-UNEE-Max problem into a feasible value that satisfies the constraints of original problem UNEE-Max in (18).

4) *Parametric subtractive transformation*: It is clear that the constraints in the Relaxed-UNEE-Max problem (20) form a convex feasible set  $\mathcal{X}$  w.r.t. the optimization variable set  $(\mathbf{p}, \mathbf{N}, \tilde{\mathbf{f}}, \mathbf{f}, \boldsymbol{\lambda}) \in \mathcal{X}$ .<sup>4</sup> However, it is still challenging due to the sum-of-ratio form in the objective [42]. To overcome this difficulty, we firstly transform the objective function in (20) into an intermediate form by introducing an auxiliary variable  $\boldsymbol{\alpha} = \{\alpha, \dots, \alpha_U\}$  and reformulate the Relaxed-UNEE-Max problem as

$$\begin{aligned}
\text{Max} \quad & \sum_{u \in \mathcal{U}} \omega_u \alpha_u \\
\text{s.t.} \quad & \frac{\sum_{k \in \mathcal{K}} \tilde{f}_{u,k}(l_u)}{\eta \sum_{k \in \mathcal{K}} p_{u,k} + P_c} \geq \alpha_u, \forall u; \\
& (\mathbf{p}, \mathbf{N}, \tilde{\mathbf{f}}, \mathbf{f}, \boldsymbol{\lambda}) \in \mathcal{X}.
\end{aligned} \tag{21}$$

Although the objective is an affine function w.r.t.  $\boldsymbol{\alpha}$ , problem (21) is not a convex optimization yet due to the fractional constraint. Thus, we further convert (21) into a parametric subtractive form and show in the following theorem its equivalence to the weighted sum maximization problem (21) with fractional constraint.

**Theorem V.1.** *Suppose  $(\mathbf{p}^*, \mathbf{N}^*, \tilde{\mathbf{f}}^*, \mathbf{f}^*, \boldsymbol{\lambda}^*, \boldsymbol{\alpha}^*)$  is the solution to problem (21), there exist  $\boldsymbol{\beta}^*$  such that for the parametric variables  $\boldsymbol{\alpha} = \boldsymbol{\alpha}^*$  and  $\boldsymbol{\beta} = \boldsymbol{\beta}^*$ ,  $(\mathbf{p}^*, \mathbf{N}^*, \tilde{\mathbf{f}}^*, \mathbf{f}^*, \boldsymbol{\lambda}^*)$  satisfies the*

<sup>4</sup>For the sake of brevity, we define the vectors of optimization variables as  $\mathbf{p} = \{p_{u,k}\}$ ,  $\mathbf{N} = \{N_{u,k}\}$ ,  $\tilde{\mathbf{f}} = \{\tilde{f}_{u,k}(l_u)\}$ ,  $\mathbf{f} = \{f_{i,j}(l_u)\}$  and  $\boldsymbol{\lambda} = \{\lambda_q\}$ .

*KKT conditions of the following problem*

$$\begin{aligned}
\text{Max} \quad & \sum_{u \in \mathcal{U}} \beta_u \left[ \sum_{k \in \mathcal{K}} \tilde{f}_{u,k}(l_u) - \alpha_u \left( \eta \sum_{k \in \mathcal{K}} p_{u,k} + P_c \right) \right] \\
\text{s.t.} \quad & (\mathbf{p}, \mathbf{N}, \tilde{\mathbf{f}}, \mathbf{f}, \boldsymbol{\lambda}) \in \mathcal{X}.
\end{aligned} \tag{22}$$

Also, the following system equations hold for the parametric variables  $(\boldsymbol{\alpha}^*, \boldsymbol{\beta}^*)$  and the tuple  $(\mathbf{p}^*, \mathbf{N}^*, \tilde{\mathbf{f}}^*, \mathbf{f}^*, \boldsymbol{\lambda}^*)$ :

$$\begin{cases} \alpha_u = \frac{\sum_{k \in \mathcal{K}} \tilde{f}_{u,k}(l_u)}{\eta \sum_{k \in \mathcal{K}} p_{u,k} + P_c} \\ \beta_u = \frac{\omega_u}{\eta \sum_{k \in \mathcal{K}} p_{u,k} + P_c}. \end{cases} \tag{23}$$

On the contrary, if  $(\mathbf{p}^*, \mathbf{N}^*, \tilde{\mathbf{f}}^*, \mathbf{f}^*, \boldsymbol{\lambda}^*)$  is the solution to problem (22) while (23) system equations are met for  $\boldsymbol{\alpha} = \boldsymbol{\alpha}^*$  and  $\boldsymbol{\beta} = \boldsymbol{\beta}^*$ , then  $(\mathbf{p}^*, \mathbf{N}^*, \tilde{\mathbf{f}}^*, \mathbf{f}^*, \boldsymbol{\lambda}^*, \boldsymbol{\alpha}^*)$  satisfies KKT conditions for problem (21), where  $\boldsymbol{\beta} = \boldsymbol{\beta}^*$  is the Lagrange multiplier for fractional constraint in (21).

*Proof.* See Appendix A. ■

Based on Theorem V.1, we can address the problem (21) by solving (22) while guaranteeing (23), such that the solution of the Relaxed-UNEE-Max could be obtained. Furthermore, it is worth noting that if the solution is unique, it is also the global solution [38]. Toward solving (22), we apply a dual-based approach, which has been widely adopted in various network settings for its simplicity of implementation, and augment it with the parametric programming to form inner loop and outer loop iterative update processes. The detailed steps are described in the following section.

## VI. ALGORITHM FOR THE RELAXED-UNEE-MAX

Based on our prior discussion, the Relaxed-UNEE-Max problem is equivalent to problem (21), whose solution is identical to (22) when satisfying (23). Hence, we focus on solving problem (22), and for the presentation clarity, we first outline the general idea of the solution algorithm.

The whole algorithm is split into an inner loop and an outer loop optimization problem. The algorithm starts with initializing the parametric variables  $\boldsymbol{\alpha}$  and  $\boldsymbol{\beta}$ . For the given  $\boldsymbol{\alpha}$  and  $\boldsymbol{\beta}$ , (22) becomes a convex optimization problem with an affine objective and a convex feasible set. The inner loop applies dual decomposition approach to solve this convex optimization problem, and each iteration of the dual-based method is termed as the inner loop iterations. Multiple inner loop iterations are performed till the optimal dual and primal solutions are reached. The output of inner loop, which is  $(\mathbf{p}^*, \mathbf{N}^*, \tilde{\mathbf{f}}^*, \mathbf{f}^*, \boldsymbol{\lambda}^*)$ , are then fed back to the outer loop to update the parametric variables  $\boldsymbol{\alpha}$  and  $\boldsymbol{\beta}$ . The overall algorithm terminates if the convergence condition for  $\boldsymbol{\alpha}$  and  $\boldsymbol{\beta}$  (we will elaborate it later) are met. Otherwise, the algorithm continues by solving the inner loop optimization problem again using the updated  $\boldsymbol{\alpha}$  and  $\boldsymbol{\beta}$ .



### A. Algorithm for The Inner Loop Optimization Problem

Suppose the parametric variables are  $\alpha^t$  and  $\beta^t$  at the  $t^{\text{th}}$  outer loop iteration, the inner loop procedure starts with introducing a partial Lagrange multiplier  $\mathbf{v} = \{v_{1,1}, \dots, v_{1,|\mathcal{K}|}, \dots, v_{U,|\mathcal{K}|}\}$  w.r.t. the third constraint (nonlinear capacity constraint) in problem (20) attempting to decouple the decision variables. We denote the partial Lagrangian by  $\mathcal{L}(\mathbf{v}; \mathbf{p}, \mathbf{N}, \tilde{\mathbf{f}}, \mathbf{f}, \lambda)$  and express it as

$$\begin{aligned} \mathcal{L}(\mathbf{v}; \mathbf{p}, \mathbf{N}, \tilde{\mathbf{f}}, \mathbf{f}, \lambda) = & \\ & \sum_{u \in \mathcal{U}} \beta_u^t \left[ \sum_{k \in \mathcal{K}} \tilde{f}_{u,k}(l_u) - \alpha_u (\eta \sum_{k \in \mathcal{K}} p_{u,k} + P_c) \right] - \\ & \sum_{u \in \mathcal{U}} \sum_{k \in \mathcal{K}} v_{u,k} \left[ \tilde{f}_{u,k}(l_u) - N_{u,k} W \log_2 \left( 1 + \frac{p_{u,k} |h_{u,k}|^2}{N_{u,k} W \cdot N_0} \right) \right]. \end{aligned} \quad (24)$$

The dual function can be then obtained as

$$\mathcal{D}(\mathbf{v}) = \max_{\mathbf{p}, \mathbf{N}, \tilde{\mathbf{f}}, \mathbf{f}, \lambda} \mathcal{L}(\mathbf{v}; \mathbf{p}, \mathbf{N}, \tilde{\mathbf{f}}, \mathbf{f}, \lambda).$$

Since problem (22) is convex and Slater's condition for constraint qualification is assumed to hold, it follows that there is no duality gap and thus the primal problem can be solved via its dual

$$\text{Relaxed-UNEE-Max Optimal} = \min_{\mathbf{v} \geq 0} \mathcal{D}(\mathbf{v}).$$

1) *Dual problem:* We solve the dual variables via the projected subgradient method. First, let us denote the primal variables obtained at  $s^{\text{th}}$  inner loop iteration as  $(\mathbf{p}^s, \mathbf{N}^s, \tilde{\mathbf{f}}^s, \mathbf{f}^s, \lambda^s)$ . Then, the dual variables at  $s^{\text{th}}$  inner loop iteration are updated as follows

$$v_{u,k}^{s+1} = \left[ v_{u,k}^s + \delta (\tilde{f}_{u,k}^s(l_u) - N_{u,k}^s W \log_2 \left( 1 + \frac{p_{u,k}^s |h_{u,k}|^2}{N_{u,k}^s W \cdot N_0} \right)) \right]^+ \quad (25)$$

where  $\delta$  is the step size and  $[\cdot]^+$  denotes the projection into the set of non-negative real numbers.

In what follows, we focus on solving the primal variables given the dual variables at each inner loop iteration.

2) *Primal problem:* We now argue that the primal problem

$$\arg \max_{\mathbf{p}, \mathbf{N}, \tilde{\mathbf{f}}, \mathbf{f}, \lambda} \mathcal{L}(\mathbf{v}^s; \mathbf{p}, \mathbf{N}, \tilde{\mathbf{f}}, \mathbf{f}, \lambda)$$

can be reorganized into a routing subproblem and a physical layer resource allocation subproblem. Thus, solving the primal problem is equivalent to solving two independent subproblems, each of which is fairly straightforward. Toward this end, we rewrite original partial Lagrangian as follows

$$\begin{aligned} \mathcal{L}(\mathbf{v}^s; \cdot) = & \underbrace{\sum_{u \in \mathcal{U}} \sum_{k \in \mathcal{K}} \left[ \beta_u^t \tilde{f}_{u,k}(l_u) - v_{u,k}^s \tilde{f}_{u,k}(l_u) \right]}_{\text{routing subproblem}} + \sum_{u \in \mathcal{U}} \left[ \right. \\ & \underbrace{\sum_{k \in \mathcal{K}} v_{u,k}^s N_{u,k} W \log_2 \left( 1 + \frac{p_{u,k} |h_{u,k}|^2}{N_{u,k} W N_0} \right) - \beta_u^t \alpha_u^t (\eta \sum_{k \in \mathcal{K}} p_{u,k} + P_c)}_{\text{resource allocation subproblem}} \left. \right] \end{aligned}$$

and we can represent it as  $\mathcal{L}(\mathbf{v}^s; \cdot) = \mathcal{L}(\mathbf{v}^s; \tilde{\mathbf{f}}, \mathbf{f}, \lambda)_{\text{rout}} + \mathcal{L}(\mathbf{v}^s; \mathbf{p}, \mathbf{N})_{\text{res}}$ . Thus, we can separate the primal optimization problem into the following subproblems

$$\begin{aligned} \text{Max } & \mathcal{L}(\mathbf{v}^s; \tilde{\mathbf{f}}, \mathbf{f}, \lambda)_{\text{rout}} \\ \text{s.t. } & \sum_{j \in \{j|i \in \mathcal{T}_j\}} f_{j,i}(l_u) + \tilde{f}_{u,i}(l_u) = \sum_{k \in \mathcal{T}_i} f_{i,k}(l_u), \forall u; \\ & \sum_{j \in \{j|b \in \mathcal{T}_j\}} f_{j,b}(l_u) = \sum_{k \in \mathcal{K}} \tilde{f}_{u,k}(l_u), \forall u; \\ & (7) \sim (8), (11), (15), (19); \\ & 0 \leq f_{i,j}(l_u), \forall l_u \in \mathcal{L}, \forall i \in \mathcal{K}, \forall j \in \mathcal{K} \setminus i. \end{aligned} \quad (26)$$

which is the routing subproblem, while

$$\begin{aligned} \text{Max } & \mathcal{L}(\mathbf{v}^s; \mathbf{p}, \mathbf{N})_{\text{res}} \\ \text{s.t. } & 0 \leq \sum_{u \in \mathcal{U}} \sum_{k \in \mathcal{K}} N_{u,k} \leq N_{\text{tot}}, N_{u,k} \in \mathbb{R}^+; \\ & 0 \leq \sum_{k \in \mathcal{K}} p_{u,k} \leq P_{u,\text{max}}, \forall u; p_{u,k} \in \mathbb{R}^+, \end{aligned} \quad (27)$$

which is the physical layer resource allocation (i.e., power control and channel allocation) subproblem.

It is clear that with the given dual variables  $\mathbf{v}^s$  and the parametric variables  $\alpha^t$  and  $\beta^t$ , the routing subproblem (26) is a linear optimization problem w.r.t. the decision variables, which can be easily solved by many softwares, such as CPLEX. On the other hand, the resource allocation subproblem belongs to the general convex optimization problem with a concave objective and a convex feasible region. Thus, it also can be easily solved via the interior point method, for instance.

With the primal variables obtained at each iteration, they are fed back to the dual variable update process according to (25), and we keep iterating the inner loop iterations till a predefined stopping criterion is met.

3) *Stopping criterion and step size:* First, we define the stopping criterion for the inner loop algorithm as  $|\mathbf{v}^{s+1} - \mathbf{v}^s| \leq \varepsilon$ , where  $\varepsilon$  denotes a predefined threshold. On the other hand, the choice of step size  $\delta$  affects the convergence rate of the solution. Normally, we could apply diminishing step size or constant but sufficiently small step size [43], which are both guaranteed to converge to the optimal solutions. We will examine the impact of step size on the convergence rate in the performance evaluation section.

### B. Algorithm for The Outer Loop Optimization Problem

The outer loop optimization problem is in a parametric subtractive form as the objective in problem (22). The goal is to iteratively obtain the parametric variables  $\alpha$  and  $\beta$ , where the iteration here is termed as the outer loop iteration. Parameter  $\alpha$  may be intuitively viewed as the ‘‘price’’ of power consumption while parameter  $\beta$  is introduced as the Lagrange multiplier for the fractional constraint in (21). Here, we apply the gradient method [20] to update the parametric variables in a following way:

$$\alpha_u^{t+1} = \alpha_u^t - \xi \left( \alpha_u^t - \frac{\sum_{k \in \mathcal{K}} \tilde{f}_{u,k}^{t,s^*}(l_u)}{\eta \sum_{k \in \mathcal{K}} p_{u,k}^{t,s^*} + P_c} \right), \forall u, \quad (28)$$

$$\beta_u^{t+1} = \beta_u^t - \xi \left( \beta_u^t - \frac{\omega_u}{\eta \sum_{k \in \mathcal{K}} p_{u,k}^{t,s^*} + P_c} \right), \forall u, \quad (29)$$

where  $\widetilde{f}_{u,k}^{t,s^*}(l_u)$  and  $p_{u,k}^{t,s^*}$  are the converged values of decision variables after  $s^*$  inner loop iterations. Similar to the inner loop optimization, another small threshold value  $\sigma$  is selected and the stopping criterion is set to  $|\alpha^{t+1} - \alpha^t| \leq \sigma$  and  $|\beta^{t+1} - \beta^t| \leq \sigma$ . The convergence of the outer loop optimization can be guaranteed by the gradient method and the step size  $\xi$  should be selected to be sufficiently small. Later, we will give the convergence analysis in the performance evaluation section.

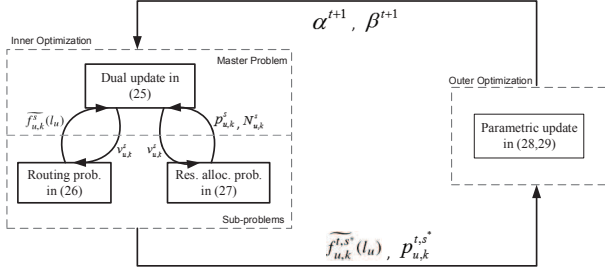


Figure 2: Summary diagram for the solution algorithm of problem (22).

For the presentation clarity, we give a high level overview of the solution algorithm for optimization problem (22) as shown in Fig.2, which shows the necessary information exchange between solution processes. Besides, Algorithm 1 formally describes the solution algorithm for the Relaxed-UNEE-Max.

---

#### Algorithm 1 Algorithm for Solving Relaxed-UNEE-Max

---

**Input:** Given network settings; Initialize all the variables  $\mathbf{p}^0, \mathbf{N}^0, \widetilde{\mathbf{f}}^0$  to any feasible value; Let  $\mathbf{v}^0 = \alpha^0 = \beta^0 = \mathbf{0}$ ; Set  $t = s = 0$ ; Initialize thresholds  $\sigma, \varepsilon$  and step size  $\delta, \xi$ .

**Output:**  $\mathbf{p}^*, \mathbf{N}^*, \widetilde{\mathbf{f}}^*, \mathbf{f}^*, \lambda^*$

- 1: Calculate  $\alpha^1, \beta^1$  and  $\mathbf{v}^1$  according to Eq.(23) and Eq.(25), respectively.
  - 2: **while**  $|\alpha^{t+1} - \alpha^t| \geq \sigma$  or  $|\beta^{t+1} - \beta^t| \geq \sigma$  **do**
  - 3:    $t \leftarrow t + 1$ ;
  - 4:   **while**  $|\mathbf{v}^{s+1} - \mathbf{v}^s| \geq \varepsilon$  **do**
  - 5:      $s \leftarrow s + 1$ ;
  - 6:     Solve resource allocation sub-problem (27) and obtain  $\mathbf{p}^s, \mathbf{N}^s$ ;
  - 7:     Solve routing sub-problem (26) and obtain  $\widetilde{\mathbf{f}}^s, \mathbf{f}^s, \lambda^s$ ;
  - 8:     Update dual variable  $\mathbf{v}^{s+1}$  according to Eq.(25);
  - 9:   **end while**
  - 10:   Update parametric variables  $\alpha^{t+1}$  and  $\beta^{t+1}$  according to Eq.(28) and Eq.(29), respectively;
  - 11: **end while**
- 

#### VII. USER ASSOCIATION AND INTEGER ROUNDING

To this end, the problem (22) is solved via the prior algorithm whose solution is identical to the one in the Relaxed-UNEE-Max problem (20). However, due to the physical

constraint that every user can only be associated with one infrastructural node, the previously obtained solution should be converted to a feasible one for the original problem. Besides, the integer property of the number of allocated OFDM sub-channels also requires a further rounding procedure to the obtained solution. Inevitably, this step could introduce performance degradation, but in the performance evaluation section, we will show that its impact on the performance is quite limited.

First, we present the association rule as

$$k = \arg \max_{i \in \mathcal{K}} \frac{\widetilde{f}_{u,i}^*(l_u)}{\eta p_{u,i}^* + P_c}, \forall u.$$

The above operation indicates that we associate the user with the infrastructural node which provides the largest value of EE. In other words, if end user  $u$  obtains the highest EE from node  $k$ , we set the association variable  $x_{u,k} = 1$  while  $x_{u,i} = 0$  for  $i \neq k$ . In so doing, we can fix the association variables and the original problem UNEE-Max in (18) could be simplified significantly. Here, we coin this simplified problem by fixing the association variables as *Asso-UNEE-Max* and it can be similarly addressed by the prior algorithm in Fig.2. In later section, the comparison between the network performance of *Asso-UNEE-Max* and the one obtained by solving *Relaxed-UNEE-Max* will be demonstrated.

Next, we introduce the integer rounding function as

$$Rnd(N_u) = \max\{\lfloor N_u \rfloor, 1\}, \forall u,$$

where the operator  $\lfloor \cdot \rfloor$  rounds the input to the greatest integer that is less than or equal to the input. Besides, the reason we apply *max* function is to guarantee that every end user can at least be assigned with one sub-channel for fairness. The rounding operation is applied to the solution obtained from solving the *Asso-UNEE-Max* problem, so that the OFDM channel allocation can be determined accordingly. However, the flow variables obtained from *Asso-UNEE-Max* may not be feasible anymore when doing integer rounding. Therefore, we need to re-solve the UNEE-Max problem (18) and get the calibrated flow values which are the feasible ones. Noticing that for the fixed channel allocation, sub-problem (27) can be easily addressed by classical iterative water-filling algorithm [44], which is just a one-dimensional (i.e., power) optimization problem. Here, we denote this solution as the one from a so-called *Rnd-UNEE-Max* problem. Its performance will be compared with the ones obtained from *Asso-UNEE-Max* and *Relaxed-UNEE-Max*, respectively, in the evaluation section.

In Algorithm 2, we formally give the detailed steps to describe the algorithm for user association and integer rounding for the outputs of Algorithm 1.

#### VIII. PERFORMANCE EVALUATION

##### A. Simulation Setup

We consider a  $500 \times 500m^2$  area served by one BS and 12 CR routers, where the BS is put in the center while CR routers represented in squares are placed around it, as shown in Fig.3. We also randomly scatter 35 end users in this area whose locations are shown by dots. The end users'

---

**Algorithm 2** Algorithm for User Association and Integer Rounding of Outputs of Algorithm 1

---

**Input:** Given the output of Algorithm 1.

**Output:** The calibrated variables  $\mathbf{p}^*, N^*, \tilde{\mathbf{f}}^*, \mathbf{f}^*, \lambda^*$

- 1: **for**  $u=1:U$  **do**
  - 2: Find  $k$  such that  $k = \arg \max_{i \in \mathcal{K}} \frac{\tilde{f}_{u,i}^*(l_u)}{\eta p_{u,i}^* + P_c}$ ;
  - 3: Set  $x_{u,k} = 1$ ;
  - 4: **end for**
  - 5: Update the problem (18) and solve the Relaxed-UNEE-Max according to Alg.1 to obtain  $\mathbf{p}', N', \tilde{\mathbf{f}}', \mathbf{f}', \lambda'$ ;
  - 6: **for**  $u=1:U$  **do**
  - 7: Let  $N_u^* = \max\{N_u', 1\}$ ;
  - 8: **end for**
  - 9: Update the problem (18) and solve the Relaxed-UNEE-Max according to Alg.1 to obtain  $\mathbf{p}^*, \tilde{\mathbf{f}}^*, \mathbf{f}^*, \lambda^*$ .
- 

devices are assumed to have an identical circuitry power consumption  $P_c = 50mW$  and power amplifier efficiency  $\eta = 5.78$ . We assume the users' allowable transmit power  $P_{u,\max}$  may vary and its impact on system performance will be examined later. To provide fairness for end users, all the weighting factors  $\omega$  are set to 1. On the infrastructure side, the CR routers are assumed to employ fixed power  $P_t$  for transmission and their antenna gain is set to  $\zeta = 4.63$ . The power interference threshold  $P_I^{th}$  is set to  $3.59 \times 10^{-7}W$  while the receiving power threshold  $P_r^{th}$  is set to  $1.0 \times 10^{-6}W$ . The transmission environment between infrastructural nodes are assumed to have path loss exponent  $n = 3$ . Given these system parameters, the interference/communication range can be calculated numerically and we could obtain the conflict graph in this regard. We utilize the OFDM channel model for wireless link between end user  $u$  and infrastructural node  $k$  as  $128.1 + 37.6 \log_{10}(r_{u,k})$  dBm where  $r_{u,k}$  is in kilometers [45]. Following the standard, we set the bandwidth of each sub-channel as  $W = 180KHz$ . The noise power spectral density is set to  $N_0 = 1 \times 10^{-12}W/Hz$ . In addition, for the harvested band, we consider that the availability of it follows a uniform distribution.

As for the algorithmic parameter settings, we set the stopping threshold  $\varepsilon$  and  $\sigma$  as 0.01 and 0.8, respectively; while the step size  $\delta = \xi = 1 \times 10^{-5}$ .

### B. Benchmark Setting

To demonstrate the advantage of our proposed ideology in improving end users' energy efficiency, we leverage the basic cellular network (i.e., 4G/LTE) as the benchmark to compare with. In other words, we consider the same end users within this geographical area served by the small cell BS as shown in Fig.3 (excluding CR routers). Similarly, the benchmark UNEE maximization problem, coined as Ben-UNEE-Max, can be

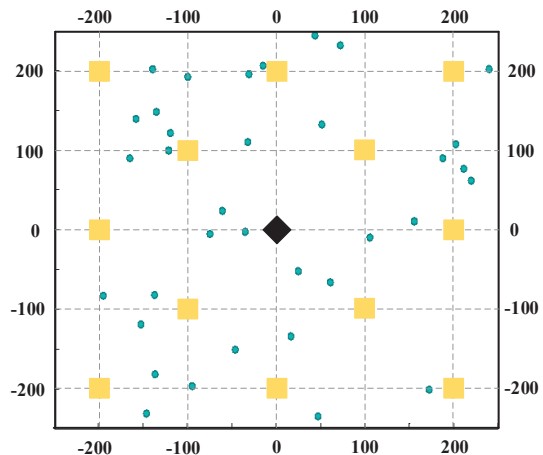


Figure 3: Evaluated network topology in an  $500 \times 500 m^2$  area: 35 end users in blue dots, 12 CR routers in yellow squares and 1 BS in black diamond.

proposed as follows:

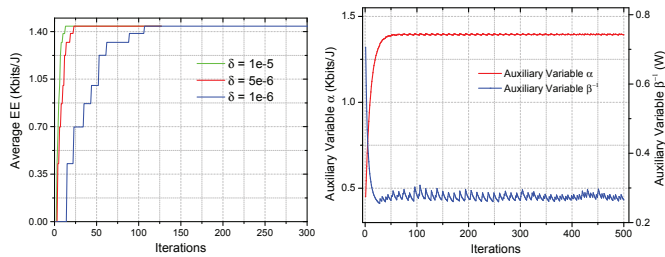
$$\begin{aligned}
 & \text{Max} \quad \sum_{u \in \mathcal{U}} \omega_u \frac{r(l_u)}{\eta p_u + P_c} \\
 & \text{s.t.} \quad \sum_{u \in \mathcal{U}} N_u \leq N_{tot}, N_u \in \mathbb{Z}^+; \\
 & \quad \quad 0 \leq r(l_u) \leq N_u W \log_2 \left( 1 + \frac{p_u |h_{u,b}|^2}{N_u W \cdot N_0} \right), \forall u \in \mathcal{U}; \\
 & \quad \quad 0 \leq p_u \leq P_{u,\max}, \forall u \in \mathcal{U}.
 \end{aligned} \tag{30}$$

In this benchmark setting, end users have to be served by the BS so the design of user association, link scheduling and flow routing is eliminated. Rather, we only consider the power control and channel allocation in this one-hop transmission scenario. To effectively solve (30), the same transformation approach can be applied to firstly convert it into a tractable one, which is then solved via the water-filling algorithm [44].

### C. Results and Analysis

First, we examine the convergence behaviors for both inner loop and outer loop optimizations. Since the inner loop is a dual-based (i.e., Lagrangian) algorithm, we also compare its convergence rate under different selection of step sizes. The results are shown in Fig.4. For demonstrative purposes, we only randomly select 10 users for this simulation and use their average EE as the metric to show the convergence performance. Here, the user's maximum allowable power  $P_{u,\max}$  is set as 1.5W while CR routers' transmit power  $P_t$  is set as 1W. The bandwidth of harvested band  $W_m$  is 100KHz and we set the confidence level  $\Delta = 0.7$ , while the number of OFDM sub-channels is selected to  $N_{tot} = 100$ . Moreover, the data in Fig.4a is collected at the last iteration of the outer loop optimization.

As we can see from Fig.4a, the average EE monotonically increases till the algorithm converges and the EE remains relatively constant (i.e., the difference not exceeding the threshold) afterwards. It can be observed that the algorithm



(a) Inner loop convergence rate under various step sizes (b) Outer loop convergence rate w.r.t. parametric variables

Figure 4: Convergence analysis for Algorithm 1

can be guaranteed to converge to the same value under three different step-size settings, but  $\delta = 1 \times 10^{-5}$  gives the fastest convergence rate (around 48 iterations). This is because as long as the step size is sufficiently small to guarantee convergence, an even smaller step size is not necessary as it slows down the rate to the optimal value. On the other hand, Fig.4b illustrates the convergence performance for the outer loop algorithm. For the notational convenience, we take the reciprocal of  $\beta$  so that its unit now becomes  $W$ , while the unit of  $\alpha$  is naturally being  $Kbits/J$  according to (23). It can be seen that the converged optimal value of  $\alpha$  is exactly the same as the one in Fig.4a, which proves the overall convergence of Algorithm 1. On the other hand, we observe that the average transmit power for end users is around  $0.28W$  at convergence, which is a small value compared to  $P_{u,max}$ .

Given the feasibility of Algorithm 1, we now conduct the performance comparison from solving Relaxed-UNEE-Max, Asso-UNEE-Max and Rnd-UNEE-Max utilizing Algorithm 1 and Algorithm 2, respectively. Besides, by solving (30), we obtain the network-wide energy efficiency in the 4G/LTE cellular network, which is used as the benchmark. The evaluation is conducted under different network sizes in terms of the number of end users. We also employ the same values of  $N_{tot}$ ,  $P_{u,max}$ ,  $W_m$  and confidence level  $\Delta$  as the previous simulation. The results are shown in Fig.5. It can be seen that these curves demonstrate the same relationship between the network size and the network-wide energy efficiency: as the number of users increase linearly, the network-wide energy efficiency first grows exponentially and then increases slowly. The reason is that the network resources in terms of OFDM sub-channels and harvested band are sufficient when the network size is small and introducing more users will increase the resource utilization efficiency, thus increasing the total network EE. As the number of users keeps increasing, the network becomes congested in the sense that scheduling and routing in the cognitive mesh network becomes the major bottleneck to further boost the network performance. In the later evaluation, we will demonstrate this phenomenon.

On the other hand, we can see that the solution to the Relaxed-UNEE-Max problem yields the highest network-wide EE since every user can be associated with several infrastructural nodes to take full advantage of network diversity. However, by fixing the association variables and solving the Asso-UNEE-Max problem does not sacrifice too much

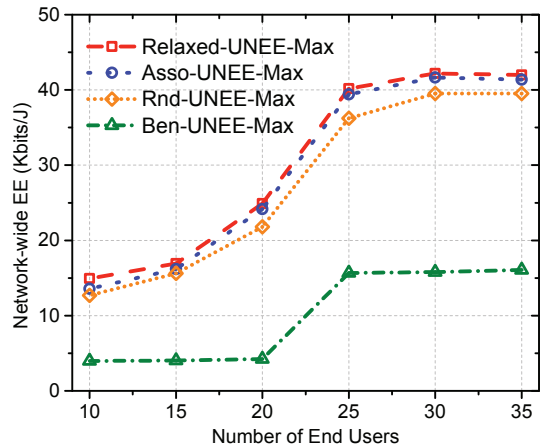
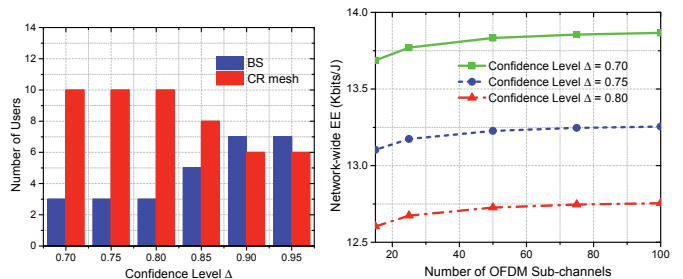


Figure 5: Performance Comparison for different problems under various network sizes.



(a) Impact of harvested band on user associations (b) Impact of number of OFDM user associations on network EE

Figure 6: Impact of bandwidth on network performance.

network performance, as shown in Fig.5. Based on the solution of the Asso-UNEE-Max problem, further applying rounding procedure and solving the Rnd-UNEE-Max problem, gives an even lower network-wide EE. Nevertheless, the optimality gaps between the solutions of Relaxed-UNEE-Max and Rnd-UNEE-Max reduces from 19.35% to 7.14% as the number of users increases from 10 to 35, which means our proposed approximation algorithm for association and rounding works well when the network size scales up.

Furthermore, the network-wide energy efficiency in our network is much higher (e.g., 143% more in the scenario of 25 end users) than that in the traditional cellular network. Such a significant gain in the energy efficiency on one hand attributes to the additional harvested spectrum while on the other hand is due to the close proximity between end users and CR routers allowing lower transmit power for users.

Next, we analyze how the number of OFDM sub-channels and uncertainty of harvested band could affect the user association decision and network performance. For the user association evaluation, we randomly select 13 users just for demonstrative purposes and set  $N_{tot} = 100$  and  $W_m = 20KHz$ , while keeping other parameters the same as before. The result is shown in Fig.6a, which illustrates the number of users connected to the BS and to the cognitive mesh network. It can be seen that when the confidence level increases, more

users are switched from the cognitive mesh network to the BS. The reason is that higher confidence level means more strict requirement on constraint (17), which in other words means that the usable harvested band becomes more limited. Therefore, some users are re-associated with the BS so that their throughput would be higher although they may use higher transmit power.

The harvested band affects the backbone capability, while the number of OFDM sub-channels impacts the capacity of the first hop from end users and infrastructural nodes. As shown in Fig.6b, we examine how different OFDM sub-channel patterns (e.g., {6, 15, 25, 50, 75, 100}) influences the network-wide EE. It can be observed that for the fixed uncertainty of the harvested band (i.e., available bandwidth), network-wide EE increases in a decreasing rate as the number of OFDM sub-channels increases. The reason is that as the number of OFDM sub-channels becomes sufficiently large, the available harvested band allocated to the cognitive mesh network becomes the bottleneck to support the traffic on the first hop links. This also explains the observation that the network-wide EE increases as the confidence level decreases for the fixed number of OFDM sub-channels.

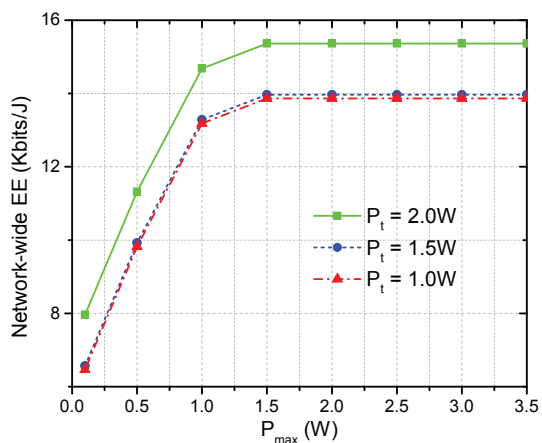


Figure 7: Impact of users' and CR routers' transmit power on network performance

Another design dimension that could impact the network performance is the transmit power. Here, we examine how the users' transmit power as well as CR routers' transmit power could jointly affect the network-wide EE. The results are shown in Fig.7. First of all, we see that the user's maximum allowable power  $P_{max}$  only affects the network-wide EE at its lower value while the network performance stays constant as  $P_{max}$  continues to increase. The reason is that end users can utilize very low power for connection and increasing the  $P_{max}$  would not give a higher transmit power in order to optimize the EE. On the other hand, the relationship between CR routers' transmit power  $P_t$  and network performance is worth explaining. According to Eq.(5-6),  $P_t$  impacts the communication/interference range, which further influences the construction of the conflict graph. For instance, when  $P_t = 1.0W$ ,  $R_i^T = 166.7m$  and  $R_i^I = 234.5m$ ; while when  $P_t = 2.0W$ ,  $R_i^T = 209.9m$  and  $R_i^I = 295.46m$ . From the

network topology shown in Fig.3, we can clearly see that the number of reachable infrastructural nodes for each CR router becomes larger while each CR router's interfered nodes remain the same. As a result, the size of each MIS  $q$  increases and more links can be scheduled for transmission at the same time, which enhances the achievable link capacity in the mesh network. Therefore, the network-wide EE increases with the  $P_t$  increasing from 1W to 2W. It should be noted that this may not always hold true if the power increase incurs more interfered nodes. However, this general trend reflects the fact that by sacrificing the infrastructure's power consumption, end users' EE will be improved, which indicates that the power consumption burden is shifted from light-weighted end devices to the more powerful infrastructural nodes.

## IX. CONCLUSION

In this work, we investigate the energy efficiency (EE) design of battery-powered devices. Our ideology is to shift their energy consumption to grid-powered devices, thus increasing their EE. This ideology is realized in a cognitive mesh network, in which we model a cross-layer optimization problem to maximize end devices' EE. Specifically, we propose an objective function as the weighted sum of each device's EE and characterize constraints including device association, flow routing, link scheduling, channel allocation and power control. To solve this complex problem, we propose parametric subtractive transformation,  $\Delta$ -confidence level, critical MISs and integer relax-then-rounding to convert the original problem into a tractable one, and further decouple this large scale optimization problem into a two-layer optimization problem. We conduct extensive simulations to demonstrate the optimality and feasibility of our proposed algorithms and also show how the design variables impact the network performance.

## REFERENCES

- [1] B. Technologies, "5 key wireless technologies for iot explained," 2017. [Online]. Available: <https://blog.bliley.com/wireless-technologies-for-iot>
- [2] S. Shea, "Iot battery outlook: Types of batteries for iot devices," 2017. [Online]. Available: <https://internetofthingsagenda.techtarget.com/feature/IoT-battery-outlook-Types-of-batt>
- [3] X. Lu, I. H. Kim, A. Xhafa, J. Zhou, and K. Tsai, "Reaching 10-years of battery life for industrial iot wireless sensor networks," in *2017 Symposium on VLSI Circuits*. IEEE, 2017, pp. C66–C67.
- [4] M. Siekkinen, M. Hienkari, J. K. Nurminen, and J. Nieminen, "How low energy is bluetooth low energy? comparative measurements with zigbee/802.15.4," in *2012 IEEE wireless communications and networking conference workshops (WCNCW)*. IEEE, 2012, pp. 232–237.
- [5] I. Juc, O. Alphand, R. Guizzetti, M. Favre, and A. Duda, "Energy consumption and performance of ieee 802.15.4e tsch and dsme," in *2016 IEEE Wireless Communications and Networking Conference*. IEEE, 2016, pp. 1–7.
- [6] R. Akeela and Y. Elziq, "Design and verification of ieee 802.11 ah for iot and m2m applications," in *2017 IEEE International Conference on Pervasive Computing and Communications Workshops (PerCom Workshops)*. IEEE, 2017, pp. 491–496.
- [7] L. Casals, B. Mir, R. Vidal, and C. Gomez, "Modeling the energy performance of lorawan," *Sensors*, vol. 17, no. 10, p. 2364, 2017.
- [8] M. R. Palattella, N. Accettura, L. A. Grieco, G. Boggia, M. Dohler, and T. Engel, "On optimal scheduling in duty-cycled industrial iot applications using ieee802.15.4e tsch," *IEEE Sensors Journal*, vol. 13, no. 10, pp. 3655–3666, 2013.
- [9] B. Reynders, W. Meert, and S. Pollin, "Power and spreading factor control in low power wide area networks," in *2017 IEEE International Conference on Communications (ICC)*. IEEE, 2017, pp. 1–6.

- [10] M. Ryan, "Bluetooth: With low energy comes low security," in *Presented as part of the 7th {USENIX} Workshop on Offensive Technologies*, 2013.
- [11] Y. Chen, S. Zhang, S. Xu, and G. Y. Li, "Fundamental trade-offs on green wireless networks," *IEEE Communications Magazine*, vol. 49, no. 6, 2011.
- [12] S. Yin, D. Chen, Q. Zhang, M. Liu, and S. Li, "Mining spectrum usage data: a large-scale spectrum measurement study," *IEEE Transactions on Mobile Computing*, vol. 11, no. 6, pp. 1033–1046, 2012.
- [13] S. Haykin, "Cognitive radio: brain-empowered wireless communications," *IEEE journal on selected areas in communications*, vol. 23, no. 2, pp. 201–220, 2005.
- [14] H. Ding, Y. Fang, X. Huang, M. Pan, P. Li, and S. Glisic, "Cognitive capacity harvesting networks: Architectural evolution towards future cognitive radio networks," *IEEE Communications Surveys & Tutorials*, 2017.
- [15] M. Centenaro, L. Vangelista, S. Saur, A. Weber, and V. Braun, "Comparison of collision-free and contention-based radio access protocols for the internet of things," *IEEE Transactions on Communications*, vol. 65, no. 9, pp. 3832–3846, 2017.
- [16] M. Polese, M. Centenaro, A. Zanella, and M. Zorzi, "M2m massive access in lte: Rach performance evaluation in a smart city scenario," in *2016 IEEE International Conference on Communications (ICC)*. IEEE, 2016, pp. 1–6.
- [17] A. Zappone, E. Jorswieck *et al.*, "Energy efficiency in wireless networks via fractional programming theory," *Foundations and Trends® in Communications and Information Theory*, vol. 11, no. 3-4, pp. 185–396, 2015.
- [18] K. T. K. Cheung, S. Yang, and L. Hanzo, "Achieving maximum energy-efficiency in multi-relay ofdma cellular networks: A fractional programming approach," *IEEE Transactions on Communications*, vol. 61, no. 7, pp. 2746–2757, 2013.
- [19] K. Xiong, P. Fan, Y. Lu, and K. B. Letaief, "Energy efficiency with proportional rate fairness in multirelay ofdm networks," *IEEE Journal on Selected Areas in Communications*, vol. 34, no. 5, pp. 1431–1447, 2016.
- [20] S. He, Y. Huang, H. Wang, S. Jin, and L. Yang, "Leakage-aware energy-efficient beamforming for heterogeneous multicell multiuser systems," *IEEE Journal on Selected Areas in Communications*, vol. 32, no. 6, pp. 1268–1281, 2014.
- [21] C. C. Zarakovitis and Q. Ni, "Maximizing energy efficiency in multiuser multicarrier broadband wireless systems: Convex relaxation and global optimization techniques," *IEEE Transactions on Vehicular Technology*, vol. 65, no. 7, pp. 5275–5286, 2016.
- [22] S. Wang, W. Shi, and C. Wang, "Energy-efficient resource management in ofdm-based cognitive radio networks under channel uncertainty," *IEEE Transactions on Communications*, vol. 63, no. 9, pp. 3092–3102, 2015.
- [23] R. Xie, F. R. Yu, H. Ji, and Y. Li, "Energy-efficient resource allocation for heterogeneous cognitive radio networks with femtocells," *IEEE Transactions on Wireless Communications*, vol. 11, no. 11, pp. 3910–3920, 2012.
- [24] S. Bayhan and F. Alagoz, "Scheduling in centralized cognitive radio networks for energy efficiency," *IEEE Transactions on Vehicular Technology*, vol. 62, no. 2, pp. 582–595, 2013.
- [25] E. Bedeer, O. Amin, O. A. Dobre, M. H. Ahmed, and K. E. Baddour, "Energy-efficient power loading for ofdm-based cognitive radio systems with channel uncertainties," *IEEE Transactions on Vehicular Technology*, vol. 64, no. 6, pp. 2672–2677, 2015.
- [26] H. Ding, C. Zhang, X. Li, J. Liu, M. Pan, Y. Fang, S. Chen, Y. Fang, C. Zhang, M. Pan *et al.*, "Session-based cooperation in cognitive radio networks: A network-level approach," *IEEE/ACM Transactions on Networking (TON)*, vol. 26, no. 2, pp. 685–698, 2018.
- [27] H. Ding, C. Zhang, Y. Cai, and Y. Fang, "Smart cities on wheels: A newly emerging vehicular cognitive capability harvesting network for data transportation," *IEEE Wireless Communications*, vol. 25, no. 2, pp. 160–169, 2017.
- [28] J. Liu, H. Ding, Y. Cai, H. Yue, Y. Fang, and S. Chen, "An energy-efficient strategy for secondary users in cooperative cognitive radio networks for green communications," *IEEE Journal on Selected Areas in Communications*, vol. 34, no. 12, pp. 3195–3207, 2016.
- [29] J. Liu, H. Yue, H. Ding, P. Si, and Y. Fang, "An energy-efficient cooperative strategy for secondary users in cognitive radio networks," in *2015 IEEE Global Communications Conference (GLOBECOM)*. IEEE, 2015, pp. 1–6.
- [30] H. G. Myung, J. Lim, and D. J. Goodman, "Single carrier fdma for uplink wireless transmission," *IEEE Vehicular Technology Magazine*, vol. 1, no. 3, pp. 30–38, 2006.
- [31] Q. Ye, B. Rong, Y. Chen, M. Al-Shalash, C. Caramanis, and J. G. Andrews, "User association for load balancing in heterogeneous cellular networks," *IEEE Transactions on Wireless Communications*, vol. 12, no. 6, pp. 2706–2716, 2013.
- [32] I. C. Wong, O. Oteri, and W. McCoy, "Optimal resource allocation in uplink sc-fdma systems," *IEEE Transactions on Wireless communications*, vol. 8, no. 5, 2009.
- [33] A. Aijaz, M. Tshangini, M. R. Nakhai, X. Chu, and A.-H. Aghvami, "Energy-efficient uplink resource allocation in lte networks with m2m/h2h co-existence under statistical qos guarantees," *IEEE Transactions on Communications*, vol. 62, no. 7, pp. 2353–2365, 2014.
- [34] D. W. K. Ng, E. S. Lo, and R. Schober, "Energy-efficient resource allocation in ofdma systems with large numbers of base station antennas," *IEEE Transactions on Wireless Communications*, vol. 11, no. 9, pp. 3292–3304, 2012.
- [35] H. Li, Y. Cheng, C. Zhou, and P. Wan, "Multi-dimensional conflict graph based computing for optimal capacity in mr-mc wireless networks," in *Distributed Computing Systems (ICDCS), 2010 IEEE 30th International Conference on*. IEEE, 2010, pp. 774–783.
- [36] T. Yucek and H. Arslan, "A survey of spectrum sensing algorithms for cognitive radio applications," *IEEE communications surveys & tutorials*, vol. 11, no. 1, pp. 116–130, 2009.
- [37] M. A. McHenry, P. A. Tenhula, D. McCloskey, D. A. Roberson, and C. S. Hood, "Chicago spectrum occupancy measurements & analysis and a long-term studies proposal," in *Proceedings of the first international workshop on Technology and policy for accessing spectrum*. ACM, 2006, p. 1.
- [38] R. W. Freund and F. Jarre, "Solving the sum-of-ratios problem by an interior-point method," *Journal of Global Optimization*, vol. 19, no. 1, pp. 83–102, 2001.
- [39] J. Borwein and A. S. Lewis, *Convex analysis and nonlinear optimization: theory and examples*. Springer Science & Business Media, 2010.
- [40] L. Liu, X. Cao, W. Shen, Y. Cheng, and L. Cai, "Dafee: A decomposed approach for energy efficient networking in multi-radio multi-channel wireless networks," in *Computer Communications, IEEE INFOCOM 2016-The 35th Annual IEEE International Conference on*. IEEE, 2016, pp. 1–9.
- [41] G. A. Holton, *Value-at-risk: theory and practice*. Academic Press New York, 2003, vol. 2.
- [42] S. Schaible and J. Shi, "Fractional programming: the sum-of-ratios case," *Optimization Methods and Software*, vol. 18, no. 2, pp. 219–229, 2003.
- [43] D. P. Bertsekas, *Nonlinear programming*. Athena scientific Belmont, 1999.
- [44] P. He, L. Zhao, S. Zhou, and Z. Niu, "Water-filling: A geometric approach and its application to solve generalized radio resource allocation problems," *IEEE transactions on Wireless Communications*, vol. 12, no. 7, pp. 3637–3647, 2013.
- [45] 3rd Generation Partnership Project (3GPP), "Further advancements for e-utra physical layer aspects, 3gpp tr 36.814," 2010, <http://www.3gpp.org/ftp/Specs/html-info/36814.htm>.

APPENDIX A  
PROOF OF THEOREM V.1

First, we re-write the FCL constraints in problem (20) using a vector form for compact representation. Given the channel model and transmit power, all the communication links among infrastructural nodes can be calculated and we use  $m$  to represent the link of an ordered node pair  $(i, j)$  while the set of links is denoted as  $\mathcal{M} = \{1, \dots, m, \dots, M\}$ . For any end user  $u$ , we can view its flow as a single-commodity model. Now, we introduce an incidence matrix  $\mathbf{A}_1 \in \mathbb{Z}^{|\mathcal{K}| \times M}$  to represent flow constraint on intermediate infrastructural nodes, where each entry  $a_{i,m}$  takes value 1 if  $i$  is the start node of link  $m$ ; -1 if  $i$  is the end node of link  $m$ ; 0 otherwise. We also present  $\mathbf{A}_2 \in \mathbb{Z}^{1 \times M}$  and  $\mathbf{A}_3 \in \mathbb{Z}^{1 \times M}$  to represent flows coming out the BS and flows aggregated at the BS from CR mesh network, respectively, where  $a_{1,m}$  is selected as 1 or 0. Thus, the FCL constraint can be re-write as follows:

$$\mathbf{A} \cdot \mathbf{f} = \mathbf{D} \cdot \tilde{\mathbf{f}}_u, \quad \forall u \in \mathcal{U} \quad (31)$$

where  $\mathbf{A} = [\mathbf{A}_1; \mathbf{A}_2; \mathbf{A}_3] \in \mathbb{Z}^{|\mathcal{K}+2| \times M}$  is the concatenation of three matrices,  $\mathbf{f} = [f_1, \dots, f_m, \dots, f_M]^T$  represents the links,  $\mathbf{D} \in \mathbb{Z}^{|\mathcal{K}+2| \times |\mathcal{K}|}$  is also an incidence matrix consisting of 1s and 0s representing the source of end user's traffic, and  $\tilde{\mathbf{f}}_u = [\tilde{f}_{u,1}, \dots, \tilde{f}_{u,k}, \dots, \tilde{f}_{u,|\mathcal{K}|}]^T$  represents the user traffic.

We introduce Lagrange multipliers  $\boldsymbol{\beta} = \{\beta_1, \dots, \beta_u, \dots, \beta_U\}$  associated with EE constraints in (21),  $\mathbf{v} = \{v_{1,1}, \dots, v_{u,1}, \dots, v_{U,|\mathcal{K}|}\}$  for capacity constraint of the link between end users and infrastructural nodes,  $\boldsymbol{\psi} = \{\psi_1, \dots, \psi_m, \dots, \psi_M\}$  for the capacity constraint (19) of the link between infrastructural nodes,  $\boldsymbol{\varphi} = \{\varphi_1, \dots, \varphi_u, \dots, \varphi_U\}$  for the transmit power constraint,  $\boldsymbol{\chi} = \{\chi_{1,1}, \dots, \chi_{1,|\mathcal{K}|+2}, \dots, \chi_{U,|\mathcal{K}|+2}\}$  associated with the FCL constraint (31) and  $\boldsymbol{\vartheta} = \{\vartheta_1, \dots, \vartheta_q, \dots, \vartheta_{Q'}\}$  for the link scheduling constraint (8). Thus, the Lagrange function of (21) is given by

$$\begin{aligned} \mathcal{L}(\mathbf{p}, N, \tilde{\mathbf{f}}, \mathbf{f}, \boldsymbol{\lambda}, \boldsymbol{\alpha}; \boldsymbol{\beta}, \mathbf{v}, \boldsymbol{\psi}, \boldsymbol{\varphi}, \boldsymbol{\chi}, \boldsymbol{\vartheta}) = & \sum_{u \in \mathcal{U}} \omega_u \alpha_u - \\ & \sum_{u \in \mathcal{U}} \beta_u [\alpha_u (\eta \sum_{k \in \mathcal{K}} p_{u,k} + P) - \sum_{k \in \mathcal{K}} \tilde{f}_{u,k}(l_u)] - \\ & \sum_{u \in \mathcal{U}} \sum_{k \in \mathcal{K}} v_{u,k} \left[ \tilde{f}_{u,k}(l_u) - N_{u,k} W \log_2 \left( 1 + \frac{p_{u,k} |h_{u,k}|^2}{N_{u,k} W \cdot N_0} \right) \right] - \\ & \sum_{m \in \mathcal{M}} \psi_m \left[ \sum_{l_u \in \mathcal{L}} f_m(l_u) - \sum_{q=1}^{Q'} \lambda_q F_{c_i,j}^{-1}(1 - \beta) \right] - \\ & \sum_{u \in \mathcal{U}} \varphi_u \left( \sum_{k \in \mathcal{K}} p_{u,k} - P_{u,\max} \right) - \sum_{u \in \mathcal{U}} \sum_{i=1}^{|\mathcal{K}|+2} \chi_{u,i} (\mathbf{a}_i \mathbf{f} - \mathbf{d}_i \tilde{\mathbf{f}}_u) \\ & - \sum_{q=1}^{Q'} \vartheta_q (\lambda_q - 1), \end{aligned} \quad (32)$$

where the  $\mathbf{a}_i = [a_{i,1}, \dots, a_{i,m}, \dots, a_{i,M}]$  is the  $i^{th}$  row of matrix  $\mathbf{A}$  and  $\mathbf{d}_i = [d_{i,1}, \dots, d_{i,k}, \dots, d_{i,|\mathcal{K}|}]$  is the  $i^{th}$  row of matrix  $\mathbf{D}$ .

Suppose  $(\mathbf{p}^*, N^*, \tilde{\mathbf{f}}^*, \mathbf{f}^*, \boldsymbol{\lambda}^*, \boldsymbol{\alpha}^*)$  are the solutions to problem (21), there exists  $\boldsymbol{\beta}^*, \mathbf{v}^*, \boldsymbol{\psi}^*, \boldsymbol{\varphi}^*, \boldsymbol{\chi}^*, \boldsymbol{\vartheta}^*$  such that the corre-

sponding KKT conditions are as follows

$$\begin{aligned} \frac{\partial \mathcal{L}}{\partial p_{u,k}} = & \beta_u^* \alpha_u^* \eta - v_{u,k}^* \frac{\partial}{\partial p_{u,k}} (N_{u,k}^* W \log_2 (1 + \frac{p_{u,k}^* |h_{u,k}|^2}{N_{u,k}^* W \cdot N_0})) \\ & - \varphi_u^* = 0, \quad \forall u, k; \end{aligned} \quad (33)$$

$$\frac{\partial \mathcal{L}}{\partial N_{u,k}} = -v_{u,k}^* \frac{\partial}{\partial N_{u,k}} (N_{u,k}^* W \log_2 (1 + \frac{p_{u,k}^* |h_{u,k}|^2}{N_{u,k}^* W N_0})) = 0, \quad \forall u, k; \quad (34)$$

$$\frac{\partial \mathcal{L}}{\partial \tilde{f}_{u,k}} = \beta_u^* - v_{u,k}^* + \chi_{u,k}^* (d_{k,k} + \sum_{i=|\mathcal{K}|+1}^{|\mathcal{K}|+2} d_{i,k}) = 0, \quad \forall u, k; \quad (35)$$

$$\frac{\partial \mathcal{L}}{\partial \lambda_q} = \sum_{m \in \mathcal{M}} \psi_m^* F_{c_m}^{-1}(1 - \beta) - \vartheta_q^* = 0, \quad q; \quad (36)$$

$$\frac{\partial \mathcal{L}}{\partial \alpha_u} = \omega_u - \beta_u^* (\eta \sum_{k \in \mathcal{K}} p_{u,k} + P) = 0 \quad \forall u; \quad (37)$$

$$\beta_u^* \frac{\partial \mathcal{L}}{\partial \beta_u} = \beta_u^* [\alpha_u^* (\eta \sum_{k \in \mathcal{K}} p_{u,k}^* + P) - \sum_{k \in \mathcal{K}} \tilde{f}_{u,k}^*] = 0, \quad \forall u; \quad (38)$$

$$v_{u,k}^* \frac{\partial \mathcal{L}}{\partial v_{u,k}} = v_{u,k}^* \left[ \tilde{f}_{u,k}^* - N_{u,k}^* W \log_2 \left( 1 + \frac{p_{u,k}^* |h_{u,k}|^2}{N_{u,k}^* W N_0} \right) \right] = 0, \quad \forall u, k; \quad (39)$$

$$\psi_m^* \frac{\partial \mathcal{L}}{\partial \psi_m} = \psi_m^* \left[ \sum_{l_u \in \mathcal{L}} f_m(l_u) - \sum_{q=1}^{Q'} \lambda_q F_{c_m}^{-1}(1 - \beta) \right] = 0, \quad \forall m; \quad (40)$$

$$\varphi_u^* \frac{\partial \mathcal{L}}{\partial \varphi_u} = \varphi_u^* (\sum_{k \in \mathcal{K}} p_{u,k} - P_{u,\max}) = 0, \quad \forall u; \quad (41)$$

$$\chi_{u,i}^* \frac{\partial \mathcal{L}}{\partial \chi_{u,i}} = \chi_{u,i}^* (a_{i,k} f_k^* - d_{i,k} \tilde{f}_{u,k}^*) = 0, \quad \forall i, u; \quad (42)$$

$$\vartheta_q^* \frac{\partial \mathcal{L}}{\partial \vartheta_q} = \vartheta_q^* (\lambda_q - 1) = 0, \quad \forall q; \quad (43)$$

Given Eq.(37) and (38) and the power consumption is a non-negative value, we can re-write them in the following forms

$$\begin{aligned} \alpha_u^* &= \frac{\sum_{k \in \mathcal{K}} \tilde{f}_{u,k}^*(l_u)}{\eta \sum_{k \in \mathcal{K}} p_{u,k}^* + P_c} \\ \beta_u^* &= \frac{\omega_u}{\eta \sum_{k \in \mathcal{K}} p_{u,k}^* + P_c} \end{aligned} \quad (44)$$

Besides, it is clear that the previous system equations are also the KKT conditions for the problem (22) given the parameters  $\alpha_u = \alpha_u^*$  and  $\beta_u = \beta_u^*$ . On the other hand, we can follow the similar procedure and prove problem (22) has the identical solution to problem (21) when (44) holds. Therefore, Theorem.V.1 is proved to be correct.